Maejo Int. J. Sci. Technol. **2017**, *11*(02), 164-174

Maejo International Journal of Science and Technology

ISSN 1905-7873
Available online at www.mijst.mju.ac.th

Full Paper

Theoretical simulation of exciton and biexciton of ZnTe/ZnS type-I and ZnTe/ZnSe type-II core/shell nanocrystals

Worasak Sukkabot

Department of Physics, Faculty of Science, Ubon Ratchathani University,
85 Sathollmark Rd., Warinchamrab, Ubon Ratchathani, Thailand, 34190
E-mail: w.sukkabot@gmail.com

Received: 30 June 2016 / Accepted: 15 August 2017 / Published: 28 August 2017

Abstract: In the present study the atomistic tight-binding theory and configuration interaction description are used to simulate the exciton and biexciton of ZnTe/ZnS type-I and ZnTe/ZnSe type-II core/shell nanocrystals. The control and tunability of the exciton and biexciton are properly engineered by the type of the band profiles and thickness of the growth shell. In particular, the exciton energies, biexciton energies, interacted coulomb integrals, exciton binding energies, biexciton binding energies, negative exciton binding energies and positive exciton binding energies are entirely sensitive to the type and dimension of the coated shells. The energies of the exciton and biexciton are reduced with the increasing growth shell thickness. In addition, the exciton and biexciton energies of ZnTe/ZnS type-I core/shell nanocrystals are greater than those of ZnTe/ZnSe type-II core/shell nanocrystals. This insight is important for a theoretical understanding and practical control by band alignments and sizes in the growth shells in order to assess the potential of particular core/shell nanocrystal structures for single exciton lasing application.

Keywords: tight-binding theory, exciton, biexciton, core/shell nanocrystal

INTRODUCTION

Studies of the exciton complexes in semiconductor core/shell nanocrystals divulge the way to the fascinating potential applications in quantum information processing, quantum communication protocols, and optical sources and detectors. Because of advances in synthesis and spectroscopy, a rich set of sharp excitonic lines in the emission spectrum is now successfully demonstrated from semiconductor core/shell nanocrystals. These lines are initiated from optical transitions between various many-carrier configurations introduced from differences between electron and hole levels. In semiconductor nanostructures there are additional principal terms of carrier-carrier repulsion, attraction and exchange, thus leading to complex configurations of the

Maejo Int. J. Sci. Technol. **2017**, *11*(02), 164-174

optical transitions. Exploiting the dependent control of the electron and hole wave functions makes it possible to adjust the exciton energies, biexciton energies and atomistic many-body electronic properties.

At the moment, the manipulation of atomistic many-body electronic behaviours in core/shell nanostructures has been divided into two main techniques, namely shell sizes and potential confinement. Sen et al. [1] theoretically studied the impact of shell structures on the exciton and biexciton binding energies in ZnSe/ZnS core/shell quantum dot using Wentzel-Kramers-Brillouin approximation. The exciton binding energy increases with increasing shell thickness until it reaches saturation at a larger shell thickness. In terms of the biexciton binding energy, there is a crossover from the bonding to anti-bonding state with increasing shell thickness for smaller core radius. Amloy et al. [2] investigated the exciton and biexciton of single GaN/Al(Ga)N quantum dots by micro-photoluminescence. They found that the biexciton binding energies are sensitive with the dot sizes. McDonald et al. [3] utilised a path-integral quantum Monte Carlo method to simulate the excitons and biexcitons in core/shell nanocrystals with type-I, type-II and quasi-type-II band alignments. In addition, Jarlov et al. [4] reported a detailed investigation of the biexciton complexes in single site-controlled pyramidal GaInAs/GaAs quantum dots using power-dependent measurements and photon correlation spectroscopy. The biexciton binding energy was found to be negative in most cases of the calculations. However, the reduction of quantum dot sizes induced the biexciton binding energy to be positive. Koc and Sahin [5] presented an exhaustive investigation of the exciton and biexciton in CdTe/CdSe type-II core/shell nanocrystals in the framework of single-band effective mass approximation. The energies of exciton and biexciton were reduced with increasing growth shell thickness.

Until now, the exciton and biexciton of semiconductor core/shell nanocrystals have been scrutinised only by simplified parabolic band models. An understanding of atomistic many-body electronic properties in the semiconductor core/shell nanocrystals essentially requires a realistic description of the atomistic detail. With an aim to accurately investigate the behaviours of the semiconductor core/shell nanocrystals, I numerically use the empirical tight-binding theory including sp^3s^* orbitals, the first nearest-neighbouring interaction, spin-orbital coupling and strain distribution. To obtain the exciton binding energy (X), biexciton binding energy (XX), negative exciton binding energy (X^-) and positive exciton binding energy (X^+), the many-body Hamiltonian is numerically solved using the configuration interaction approach [6-9]. In the present computations, ZnTe cores terminated with various monolayers of ZnS and ZnSe shells are the simulated candidates, thus forming ZnTe/ZnS type-I and ZnTe/ZnSe type-II core/shell nanocrystals.

Lincheneau et al. [10] presented a synthesis of spherical ZnTe nanocrystals and a successive coating with ZnS shell as the core/shell nanocrystals. A Type-I band alignment was demonstrated in the ZnTe/ZnS core/shell nanocrystals. The ZnS shell could enhance the chemical and photochemical stability of these core/shell nanocrystals, thus representing an alternative to cadmium-free nanostructures for optoelectronic applications. In addition, Fairclough et al. [11] reported the structural and optical properties of type-II ZnTe/ZnSe core/shell nanocrystals. The optical band gaps were tuned across the visible spectrum by changing the growth shell thickness. To analyse the effect of the growth shell thickness and band profiles on the atomistic many-body electronic behaviours, the exciton energies, biexciton energies, coulomb integrals, X, XX, X^- and X^+ with different growth shell thicknesses and band alignments were computed using the atomistic tight-binding theory and configuration interaction method.

Maejo Int. J. Sci. Technol. **2017**, *11*(02), 164-174

In this paper the prediction of exciton and biexciton of ZnTe/ZnS type-I and ZnTe/ZnSe type-II core/shell nanocrystals is numerically presented as a function of the growth shell thickness using the atomistic tight-binding theory and configuration interaction method. The next section briefly describes the procedure for the computations. In the third section the results are reported with the purpose of demonstrating the dependence of the coated shell thickness and band alignments on the exciton, biexciton and interacted binding energies.

METHODS

In the following, a systematic study of ZnTe core surrounded by either ZnS or ZnSe shell as a function of the growth shell thickness is presented. The aim is to theoretically examine the impact of shell size and band profile on the atomistic many-body electronic properties of the studied semiconductor core/shell nanocrystals. To do so, there are three main steps in the analysis of the atomistic many-body electronic behaviours. In the beginning, there is a lattice mismatch between the core material (ZnTe) and the shell material (ZnS or ZnSe). To obtain the strained atomic positions, I use the atomistic valence force field. [12-15] The elastic energy of all atoms is expressed as a function of the atomic positions R_i as

$$E=\sum_i \sum_{j=1}^{4} \frac{3\alpha_{ij}}{16(d_{ij}^0)^2}[(R_j - R_i)^2 - (d_{ij}^0)^2]^2 + \sum_i \sum_{j,k>1}^{4} \frac{3\beta_{ijk}}{8d_{ij}^0 d_{ik}^0}[(R_j - R_i)\cdot(R_k - R_i) - \cos\theta d_{ij}^0 d_{ik}^0]^2 \cdot$$

Here, d_{ij}^0 denotes the bulk equilibrial bond length between the nearest-neighbouring atom i and j in the corresponding binary compound and $\theta = \arccos(1/3)$ is the ideal bond angle. The first term is the sum over all atoms i and their nearest neighbours j. The second term is the sum over all atoms i and distinct pairs of their nearest neighbours j and k. There are two empirical force constants (α and β) used in the atomistic valence force field. These parameters are fitted to reproduce the bulk elastic properties (C_{11}, C_{12} and C_{44} bulk elastic constants).

In the second step of the calculation the single-particle states are obtained by building the sp^3s^* tight-binding Hamiltonian [16] and then diagonalising it to obtain single-particle energies and states. This technique has been effectively used for studying structural and optical properties of semiconductor core/shell nanocrystals [14, 15, 17-20]. The single-particle tight-binding Hamiltonian is written in the language of second quantisation in the following form:

$$H_{TB} = \sum_{R=1}^{N_{at}} \sum_{\alpha=1}^{10} \varepsilon_{R\alpha} c_{R\alpha}^{\dagger} c_{R\alpha} + \sum_{R=1}^{N_{at}} \sum_{\alpha=1}^{10} \sum_{\alpha'=1}^{10} \lambda_{R\alpha\alpha'} c_{R\alpha}^{\dagger} c_{R\alpha'} + \sum_{R=1}^{N_{at}} \sum_{R'=1}^{N_{at}} \sum_{\alpha=1}^{10} \sum_{\alpha'=1}^{10} t_{R\alpha,R'\alpha'} c_{R\alpha}^{\dagger} c_{R'\alpha'} \ ,$$

where the operator $c_{R\alpha}^{\dagger}(c_{R\alpha})$ creates (or annihilates) particle on the orbital α of atom R. The on-site orbital energies $\varepsilon_{R\alpha}$, the spin-orbit coupling constant $\lambda_{R\alpha\alpha'}$ and the hopping matrix elements $t_{R\alpha,R'\alpha'}$ are empirical parameters. The inclusion of spin-orbital coupling into the tight-binding model introduces an additional parameter λ as described by Chadi. [21]. Here, I employ the parameterisation [22] of ZnTe, ZnS and ZnSe, which is fitted to provide experimental bulk band structures, determined bulk transition energies and effective masses. To obtain single-particle spectra, I implement PReconditioned Iterative MultiMethod Eigensolver [23, 24] to numerically diagonalise the matrix of tight-binding Hamiltonian (H_{TB}).

Maejo Int. J. Sci. Technol. **2017**, *11*(02), 164-174

In the final step the many-body Hamiltonian for interacting electrons and holes is written in the second quantisation expressed as

$$H = \sum_i E_i e_i^\dagger e_i + \sum_j E_j h_j^\dagger h_j + \frac{1}{2}\sum_{ijkl} V_{ijkl}^{ee,coul} e_i^\dagger e_j^\dagger e_k e_l +$$
$$\frac{1}{2}\sum_{ijkl} V_{ijkl}^{hh,coul} h_i^\dagger h_j^\dagger h_k h_l - \sum_{ijkl} V_{ijkl}^{eh,coul} h_i^\dagger e_j^\dagger e_k h_l + \sum_{ijkl} V_{ijkl}^{eh,exch} h_i^\dagger e_j^\dagger e_k h_l$$

The first two terms are the single-particle energies of electron and hole states respectively. The third and fourth terms describe the electron-electron and hole-hole coulomb interactions respectively. The fifth and sixth terms represent the electron-hole coulomb and exchange interactions respectively. The many-body Hamiltonian for X, XX, X^- and X^+ is solved using the so-called configuration interaction approach [6-9].

RESULTS AND DISCUSSION

In the present computations the ZnTe core terminated by ZnS or ZnSe coated shell is utilised as a computational model. According the potential confinement, ZnTe/ZnS and ZnTe/ZnSe core/shell nanocrystals display type-I and type-II band profiles respectively. According to Lincheneau et al. [10] and Fairclough et al. [11], the range of ZnTe core in ZnTe/ZnS and ZnTe/ZnSe core/shell nanocrystals is 3.6-6.1 nm. Here, the increasing shell thicknesses of ZnS and ZnSe growth shell are grown on a ZnTe core with a fixed diameter of 4.00 nm. The definition of a monolayer (ML) is a shell of ZnS that exhibits an average thickness of 0.31 nm. [25] To theoretically analyse the impact of the coated shell thickness and band profile on the exciton energies, biexciton energies, X, XX, X^- and X^+, I implement a combination of the atomistic tight-binding theory and configuration interaction method to achieve the objective.

The present study is expected to provide potential implementation of the core/shell nanocrystals as a single exciton lasing application [26-28]. Therefore, the understanding of atomistic many-body electronic properties is important. Figure 1 plots the exciton and biexciton energies with different types of coated shells and shell thicknesses. As expected, increasing coated shell thickness from 0 ML to 5 ML reduces the energies of the exciton and biexciton of ZnTe/ZnS type-I core/shell nanocrystals as described by the quantum confinement. Also, the energies of the exciton and biexciton of ZnTe/ZnSe type-II core/shell nanocrystals are decreased because of the weak binding energies induced by increasing exciton radii. Besides, the energies of the biexciton are greater than those of the exciton. Surprisingly, the exciton and biexciton energies of ZnTe/ZnS type-I core/shell nanocrystals are greater than those of ZnTe/ZnSe type-II core/shell nanocrystals due to the dependence of the band profiles on exciton and biexciton energies. With increasing growth shell thickness, the discrepancies between biexciton and exciton energies are more pronounced. Therefore, one can practically tune the exciton and biexciton energies by introducing and varying the type and dimensions of the growth shell.

Maejo Int. J. Sci. Technol. **2017**, *11*(02), 164-174

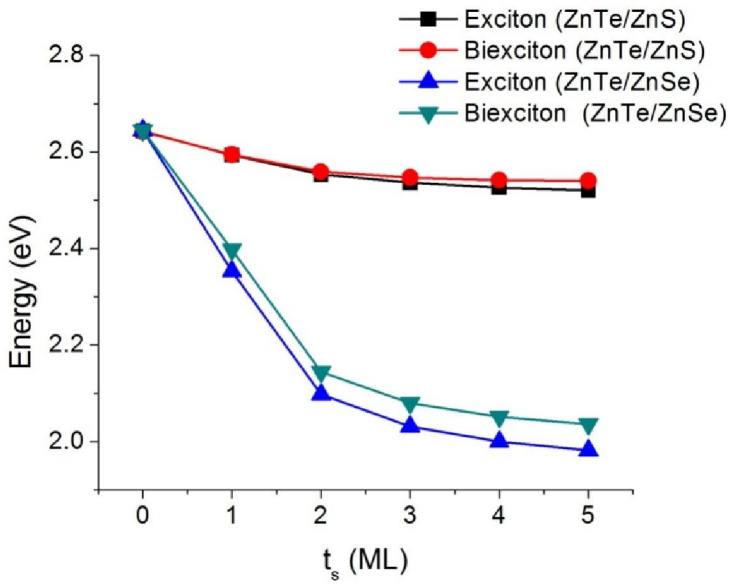

Figure 1. Exciton and biexciton energies of ZnTe/ZnS type-I and ZnTe/ZnSe type-II core/shell nanocrystals as a function of growth shell thickness (t_s)

Next, Figure 2 shows electron-electron (J_{ee}), electron-hole (J_{eh}) and hole-hole (J_{hh}) coulomb integrals calculated for electron and hole occupying their ground state of ZnTe/ZnS type-I and ZnTe/ZnSe core/shell nanocrystals. As is well known, the reduction of J_{ee}, J_{eh} and J_{hh} is demonstrated with increasing growth shell thickness. This means that the electron-electron, electron-hole and hole-hole interactions, localised in the studied core/shell nanocrystals, are decreased in thicker coated shells. In the absence of growth shell, there is no effect on J_{ee} or J_{hh}, except on J_{eh}. In the presence of growth shell, the coulomb integrals normally change. This characteristic ordering of atomistic many-body interactions with increasing energies—J_{hh}, J_{eh} and J_{ee}—is demonstrated. The interaction between hole and hole is largest and not sensitive to the coating layer thickness because the holes are localised within the fixed ZnTe core. The electron and hole are confined in the ZnTe core in ZnTe/ZnS type-I core/shell nanocrystals, while electron and hole are localised in the ZnSe shell and ZnTe core respectively in ZnTe/ZnSe type-II core/shell nanocrystals. Therefore, the electron-electron and hole-hole interactions in ZnTe/ZnS type-I core/shell nanocrystals are greater than those in ZnTe/ZnSe type-II core/shell nanocrystals. The electron-hole interaction in the former is greater than one in the latter because electrons and holes in the former nanocrystals are confined in the same ZnTe core regime. Thus, the atomistic many-body electronic properties localised in the investigated core/shell nanocrystals are controlled by means of the band alignments and sizes in the passivated shell.

Maejo Int. J. Sci. Technol. **2017**, *11*(02), 164-174

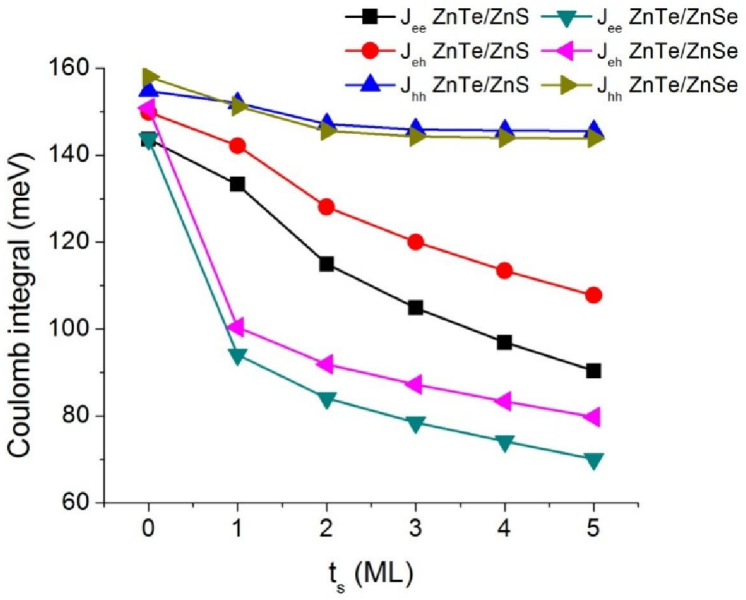

Figure 2. Ground-state coulomb integrals (J) of ZnTe/ZnS type-I and ZnTe/ZnSe type-II core/shell nanocrystals as a function of growth shell thickness (t_s)

After studying the exciton energies, biexciton energies and coulomb integrals, an attempt is made to control their binding energies, in particular with the growth shell thickness and band profiles. The X of a bulk ZnTe semiconductor is about 13.00 meV [29, 30]. Because of the quantum confinement, the X of the ZnTe nanocrystal is significantly improved. Figures 3, 4, 5 and 6 show the X, XX, X^- and X^+ respectively as a function of growth shell thickness. They are numerically measured with respect to the exciton energy. The computations suggest that X, XX and X^+ are unbound (have positive binding energy) but X^- is bound. In the absence of the growth shell, the findings show that the biexciton anti-binding appears (negative). However, the growth shells induce the biexciton binding (positive) in all cases. In the presence of the coated shell, X and X^- are decreased, while XX and X^+ are increased. With increasing growth shell thickness, X and X^- are reduced but XX and X^+ are increased. In addition, the X of ZnTe/ZnS type-I core/shell nanocrystals is greater than that of ZnTe/ZnSe type-II core/shell nanocrystals as described by J_{eh} terms. However, the XX, X^- and X^+ of the latter nanocrystals are greater than those of the former. Therefore, the many-body binding energies are practically controlled by the size of the terminated shell and the type of the band alignments.

Maejo Int. J. Sci. Technol. **2017**, *11*(02), 164-174

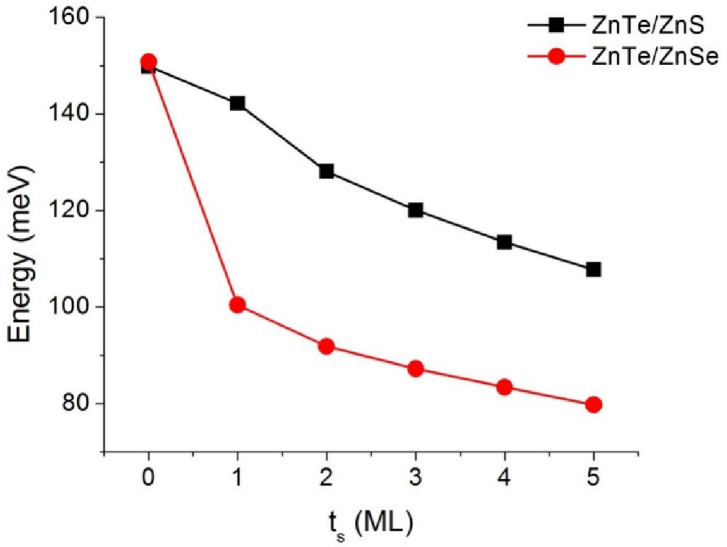

Figure 3. Exciton binding energies (X) of ZnTe/ZnS type-I and ZnTe/ZnSe type-II core/shell nanocrystals as a function of growth shell thickness (t_s)

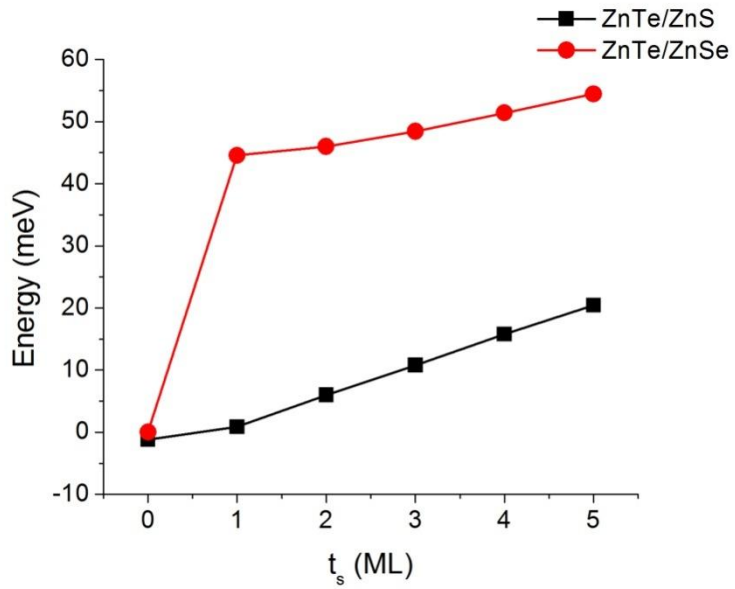

Figure 4. Biexciton binding energies (XX) of ZnTe/ZnS type-I and ZnTe/ZnSe type-II core/shell nanocrystals as a function of growth shell thickness (t_s)

Maejo Int. J. Sci. Technol. **2017**, *11*(02), 164-174

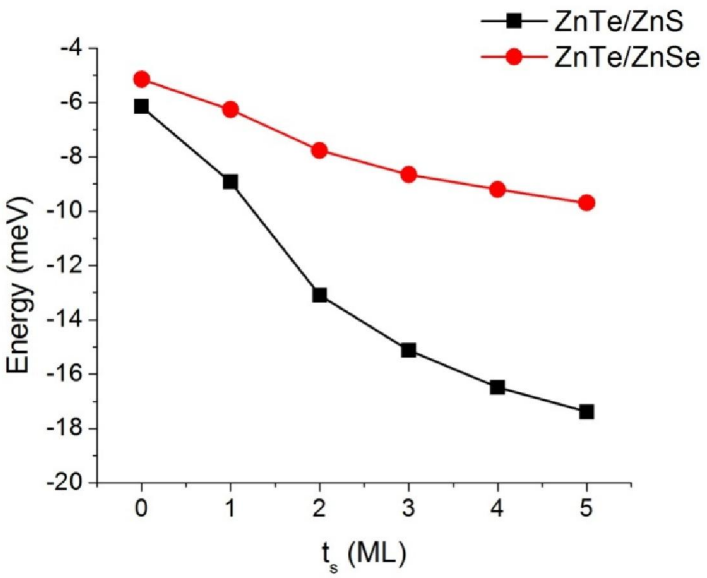

Figure 5. Negative exciton binding energies (X^-) of ZnTe/ZnS type-I and ZnTe/ZnSe type-II core/shell nanocrystals as a function of growth shell thickness (t_s)

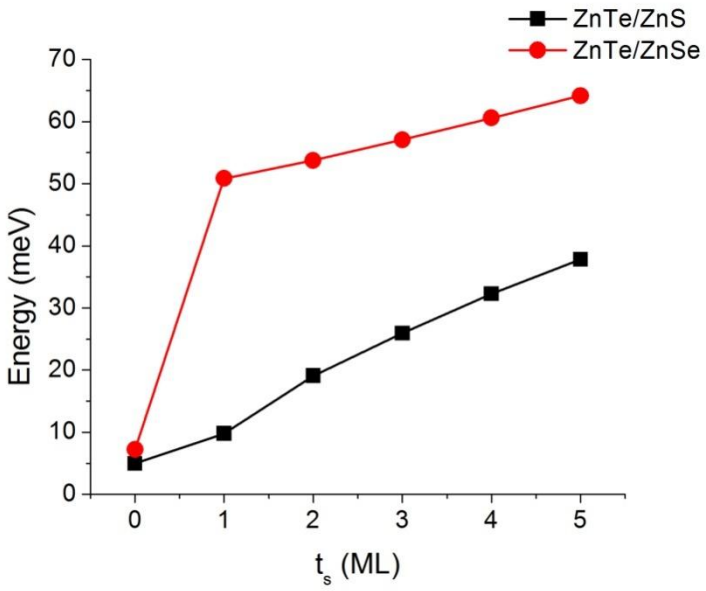

Figure 6. Positive exciton binding energies (X^+) of ZnTe/ZnS type-I and ZnTe/ZnSe type-II core/shell nanocrystals as a function of growth shell thickness (t_s)

CONCLUSIONS

Detailed information on atomistic many-body electronic properties in ZnTe/ZnS type-I and ZnTe/ZnSe type-II core/shell nanocrystals has been acquired by theoretical simulation using atomistic tight-binding theory and configuration interaction description. The manipulation of atomistic many-body electronic behaviours has been accomplished by changing the growth shell thickness and type of band alignments. Increasing coated shell thickness reduces the energies of the exciton and biexciton of ZnTe/ZnS type-I core/shell nanocrystals described by quantum confinement, while the decreased energies of the exciton and biexciton of ZnTe/ZnSe type-II

core/shell nanocrystals are described by weak binding energies as confirmed by the increased exciton radii. The exciton and biexciton energies of ZnTe/ZnS type-I core/shell nanocrystals are greater than those of ZnTe/ZnSe type-II core/shell nanocrystals. In addition, the electron-electron, electron-hole and hole-hole interactions in the former nanocrystals are greater than those in the latter nanocrystals. With increasing growth shell thickness, X and X^- are reduced but XX and X^+ are increased. The X of ZnTe/ZnS type-I core/shell nanocrystals is greater than that of ZnTe/ZnSe type-II core/shell nanocrystals, while the XX, X^- and X^+ of the type-II nanocrystals are greater than those of the type-I nanocrystals. Finally, the manipulation of atomistic many-body electronic properties by means of growth shell thickness and band profiles allows an assessing of particular semiconductor core/shell nanocrystal structures for single exciton laser implementation.

ACKNOWLEDGEMENTS

The author gratefully acknowledges the financial support from the Thailand Research Fund Grants (TRG58880072) and Department of Physics, Faculty of Science, Ubon Ratchathani University.

REFERENCES

1. P. Sen, S. Chattopadhyay, J. T. Andrews and P. K. Sen, "Impact of shell thickness on exciton and biexciton binding energies of a ZnSe/ZnS core-shell quantum dot", *J. Phys. Chem. Solids*, **2010**, *71*, 1201-1205.
2. S. Amloy, K. H. Yu, K. F. Karlsson, R. Farivar, T. G. Andersson and P. O. Holtz, "Size dependent biexciton binding energies in GaN quantum dots", *Appl. Phys. Lett.*, **2011**, *99*, 251903-251905.
3. P. G. McDonald, E. J. Tyrrell, J. Shumway, J. M. Smith and I. Galbraith, "Tuning biexciton binding and anti-binding in core/shell quantum dots", *Phys. Rev. B.*, **2012**, *86*, 125310-125318.
4. C. Jarlov, P. Gallo, M. Calic, B. Dwir, A. Rudra and E. Kapon, "Bound and anti-bound biexciton in site-controlled pyramidal GaInAs/GaAs quantum dots", *Appl. Phys. Lett.*, **2012**, *101*, 191101-191104.
5. F. Koc and M. Sahin, "Electronic and optical properties of single excitons and biexcitons in type-II quantum dot nanocrystals", *J. Appl. Phys.*, **2014**, *115*, 193701-193710.
6. J. W. Luo, A. Franceschetti and A. Zunger, "Nonmonotonic size dependence of the dark/bright exciton splitting in GaAs nanocrystals", *Phys. Rev. B.*, **2009**, *79*, 201301-201304.
7. G. Bester, S. Nair and A. Zunger, "Pseudopotential calculation of the excitonic fine structure of million-atom self-assembled $In_{1-x}Ga_xAs$/GaAs quantum dots", *Phys. Rev. B.*, **2003**, *67*, 161306-161309.
8. M. Korkusinski and P. Hawrylak, "Atomistic theory of emission from dark excitons in self-assembled quantum dots", *Phys. Rev. B.*, **2013**, *87*, 115310-115320.
9. M. Zieliński, "Valence band offset, strain and shape effects on confined states in self-assembled InAs/InP and InAs/GaAs quantum dots", *J. Phys. Condens. Matter*, **2013**, *25*, 465301- 465317.
10. C. Lincheneau, M. Amelia, M. Oszajca, A. Boccia, F. D'Orazi, M. Madrigale, R. Zanoni, R. Mazzaro, L. Ortolani, V. Morandi, S. Silvi, K. Szaciłowski and A. Credi, "Synthesis and properties of ZnTe and ZnTe/ZnS core/shell semiconductor nanocrystals", *J. Mater. Chem. C*, **2014**, *2*, 2877-2886.

11. S. M. Fairclough, E. J. Tyrrell, D. M. Graham, P. J. B. Lunt, S. J. O. Hardman, A. Pietzsch, F. Hennies, J. Moghal, W. R. Flavell, A. A. R. Watt and J. M. Smith, "Growth and characterization of strained and alloyed type-II ZnTe/ZnSe core-shell nanocrystals", *J. Phys. Chem. C*, **2012**, *116*, 26898-26907.
12. P. N. Keating, "Effect of invariance requirements on the elastic strain energy of crystals with application to the diamond structure", *Phys. Rev.*, **1996**, *145*, 637-645.
13. R. M. Martin, "Elastic properties of ZnS structure semiconductors", *Phys. Rev. B.*, **1970**, *1*, 4005- 4011.
14. W. Sukkabot, "Variation in the structural and optical properties of CdSe/ZnS core/shell nanocrystals with ratios between core and shell radius", *Phys. B Condens. Matter*, **2014**, *454*, 23-30.
15. W. Sukkabot, "Electronic structure and optical properties of colloidal InAs/InP core/shell nanocrystals: Tight-binding calculations", *Phys. E Low Dimension. Syst. Nanostruct.*, **2014**, *63*, 235-240.
16. P. Vogl, H. P. Hjalmarson and J. D. Dow, "A semi-empirical tight-binding theory of the electronic structure of semiconductors", *J. Phys. Chem. Solids*, **1983**, *44*, 365-378.
17. W. Sukkabot, "Influence of ZnSe core on the structural and optical properties of ZnSe/ZnS core/shell nanocrystals: Tight-binding theory", *Superlatt. Microstruct.*, **2014**, *75*, 739-748.
18. W. Sukkabot, "Tight-binding study of the manipulation of the structural and optical properties in cadmium selenide/zinc sulfide core/shell nanocrystals with shell thickness", *Mater. Sci. Semiconduct. Process.*, **2014**, *27*, 1020-1027.
19. W. Sukkabot, "Atomistic tight-binding theory in CdSe/ZnSe wurtzite core/shell nanocrystals", *Comput. Mater. Sci.*, **2015**, *96*, 336-341.
20. W. Sukkabot, "Effect of ZnS shell on tight-binding simulation of zinc-blende ZnTe/ZnS core/shell nanocrystals", *Comput. Mater. Sci.*, **2015**, *101*, 275-280.
21. D. J. Chadi, "Spin-orbit splitting in crystalline and compositionally disordered semiconductors", *Phys. Rev. B.*, **1977**, *16*, 790-796.
22. D. Olguin, R. Baquero and R. de Coss, "The band gap of II-VI ternary alloys in a tight-binding description", *Rev. Mexica. Fisica*, **2001**, *47*, 43-49.
23. A. Stathopoulos and J. R. McCombs, "PRIMME: PReconditioned iterative multimethod eigensolver: Methods and software description", *ACM Trans. Math. Software*, **2010**, *37*, 1-29.
24. L. Wu, E. Romero and A. Stathopoulos, "PRIMME_SVDS: A high-performance preconditioned SVD solver for accurate large-scale computations", *arXiv*:1607.01404 (**2016**).
25. D. Chen, F. Zhao, H. Qi, M. Rutherford and X. Peng, "Bright and stable purple/blue emitting CdS/ZnS core/shell nanocrystals grown by thermal cycling using a single-source precursor", *Chem. Mater.*, **2010**, *22*, 1437-1444.
26. C. Grivas, C. Li, P. Andreakou, P. Wang, M. Ding, G. Brambilla, L. Manna and P. Lagoudakis, "Single-mode tunable laser emission in the single-exciton regime from colloidal nanocrystals", *Nature Comm.*, **2013**, doi:10.1038/ncomms3376.
27. N. Horiuchi, "Colloidal nanocrystals: Single-exciton lasing", *Nature Nanotech.*, **2012**, *7*, 335-339.
28. V. I. Klimov, S. A. Ivanov, J. Nanda, M. Achermann, I. Bezel, J. A. McGuire and A. Piryatinski, "Single-exciton optical gain in semiconductor nanocrystals", *Nature*, **2007**, *447*, 441- 446.

Maejo Int. J. Sci. Technol. **2017**, *11*(02), 164-174

29. A. Naumov, K. Wolf, T. Reisinger, H. Stanzl and W. Gebhardt, "Luminescence due to lattice-mismatch defects in ZnTe layers grown by metalorganic vapor phase epitaxy", *J. Appl. Phys.*, **1993**, *73*, 2581-2583.
30. Y. Zhang, B. J. Skromme and F. S. Tucro-Sandroff, "Effects of thermal strain on the optical properties of heteroepitaxial ZnTe", *Phys. Rev. B.*, **1992**, *46*, 3872-3885.

© 2017 by Maejo University, San Sai, Chiang Mai, 50290 Thailand. Reproduction is permitted for noncommercial purposes.